ISSN 1995-0780, Nanotechnologies in Russia, 2018, Vol. 13, Nos. 3–4, pp. 152–160. © Pleiades Publishing, Ltd., 2018.
Original Russian Text © E.A. Eremina, A.V. Kaplin, A.A. Eliseev, A.V. Sidorov, Sh.S. Radzhabzoda, A.V. Grigor'eva, E.A. Gudilin, 2018, published in Rossiiskie Nanotekhnologii, 2018, Vol. 13, Nos. 3–4.

NANOBIOLOGY

Multifunctional Composites Based on Graphite Oxide, Doxorubicin, and Magnetic Nanoparticles for Targeted Drug Delivery

E. A. Eremina[a]*, A. V. Kaplin[a], A. A. Eliseev[b], A. V. Sidorov[b], Sh. S. Radzhabzoda[b], A. V. Grigor'eva[a, b], and E. A. Gudilin[a, b]

[a] *Faculty of Chemistry, Moscow State University, Moscow, 119992 Russia*
[b] *Faculty of Materials Science, Moscow State University, Moscow, 119992 Russia*
**e-mail: ea_er@mail.ru*

Received September 27, 2017; in final form, March 12, 2018

Abstract—This work is dedicated to the synthesis of a GO@Fe_3O_4@DOX multifunctional nanocomposite composed of graphite oxide, superparamagnetic iron oxide nanoparticles, and the drug doxorubicin. The final product combines double magnetic and molecular targeting to tumor tissues. Superparamagnetic Fe_3O_4 nanoparticles are first chemically deposited onto a surface of graphite oxide (GO) with the acquisition of a double GO@Fe_3O_4 composite. The material is then bound with the antitumor drug doxorubicin. The morphology, phase composition, and magnetic and optical properties of synthesized samples are characterized via thermal gravimetry, X-ray diffraction, magnetic susceptibility measurements, transmission electron microscopy, and via UV-visible and Raman spectroscopy. The optimal ratio of graphite oxide, iron oxide, and doxorubicin for the creation of a potential precursor of the new drug is established. The presence of doxorubicin and iron oxide in the composite is confirmed, making it possible to use an external magnetic field for targeted drug delivery towards the affected tissues. It is also shown that the composite retains its stability for a month in solutions with physiological pH values.

DOI: 10.1134/S1995078018020027

The development of new methods for the targeted delivery of drugs will substantially improve the safety and efficiency of their therapeutic effect. Materials based on graphene and its derivatives, such as graphene oxide, seem promising for solving this problem, whose extensive study has been initiated by Geim and Novoselov [1]. Due to the unique honeycomb-like structure composed of single layers of sp^2 hybridized carbon atoms, graphene possesses excellent heat and electric conductivity, a large specific surface, and biocompatibility [2–6]. Graphene and its derivatives contain the 6-atom layers with a system of conjugate π bonds, enabling one to refer to these compounds as planar aromatic macromolecules whose surface can be immobilized with various macromolecular substances, including drugs, noble metals, and magnetic materials in the form of nanoparticles [7–12]. The presence of various oxygen-containing functional groups (–COOH, –COH, –OH, =O), formed during the chemical synthesis of graphene and graphite oxide on the surface, favor the construction of chemical bonds between a carbonaceous material and a DOX drug containing the $-NH_2$ aminogroups.

An antracycline antibiotic—doxorubicin ($C_{27}H_{29}NO_{11}$)—is used extensively in the treatment of oncological diseases (Fig. 1). Nevertheless, its clinical application is limited because of the noticeable side effects caused by cardiotoxicity. The targeted delivery of the medicament to the affected organ will allow one to use smaller doses of the drug and, consequently, to reduce side effects. This task can be solved through the synthesis of composites that contain doxorubicin, superparamagnetic iron oxide nanoparticles, and graphite oxide.

A molecule of doxorubicin, including the aminogroup, is able to form a chelate complex with iron oxide [13–17], which ensures strong chemical cou-

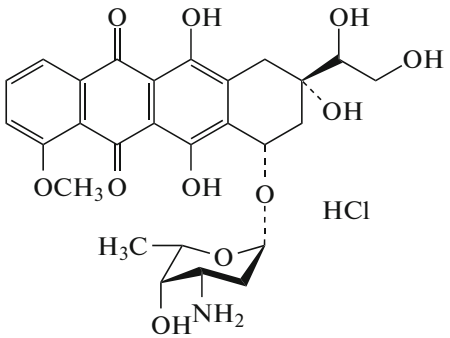

Fig. 1. Doxorubicin molecule.

Table 1. Compositions and volumes of iron oxide and doxorubicin solutions

Composition of DOX@Fe_3O_4, wt %	Fe_3O_4 nanoparticle solution volume (0.012 g/mL), μL	DOX solution volume (1 mg/μL in phosphate buffer), μL
82% DOX–18% Fe_3O_4	14220	780
75% DOX–25% Fe_3O_4	14477	523
50% DOX–50% Fe_3O_4	14820	180

pling. The presence of superparamagnetic properties in iron oxide nanoparticles will enable one to use the external magnetic field for delivering the drug to the affected organ.

The presence of graphite oxide in the composite, which has a planar structure and developed surface, will allow a large amount of iron oxide chemically coupled with DOX to be sorbed on its surface. Furthermore, oxygen-containing functional groups onto the GO surface favor the additional formation of chemical bonds between the aminogroups of doxorubicin molecule and the carboxyl groups of GO.

This work is aimed at designing a multifunctional structure that combines the double magnetic and molecular targeting to tumor tissues. Superparamagnetic Fe_3O_4 nanoparticles were chemically deposited onto the GO surface with the formation of GO@Fe_3O_4 nanocomposites. The successive coupling of the material with doxorubicin (DOX) resulted in the final GO@Fe_3O_4@DOX composite.

EXPERIMENTAL

Reagents. Reagents were medium-flake graphite, $KMnO_4$ (chemically pure), H_2SO_4 (concentrated chemically pure), H_3PO_4 (85%, chemically pure), H_2O_2 (30%), $Na_3C_6H_5O_7$ sodium citrate (chemically pure), NH_3 (concentrated), H_2O (distilled), C_2H_5OH (Ferein, 95%), $H_2C_2O_4$ (pure), $FeSO_4 \cdot 7H_2O$ (chemically pure), $FeCl_3 \cdot 6H_2O$ (pure), doxorubicin hydrochloride (TEVA, Netherlands), and phosphate buffer solution with pH 7.5.

Preparation of the buffer solution. A buffer solution of 50 mM KH_2PO_4 and 2 mM $MgSO_4$ was used. It was prepared in 1 L of distilled water by solving 6.85 g of KH_2PO_4 and 0.24 g of $MgSO_4$. The pH of the solution was adjusted to a value of 7.5 with dry KOH sodium hydroxide pellets (approximately 8 pellers or 1.7 g). The buffer solution was stored at a temperature of +4°C, allowing one to maintain its stability for 1–2 months.

Synthesis of graphite oxide. Graphite oxide was synthesized in accordance with the improved Hammers method [5]. For this purpose, 1.5 g of medium-flake graphite was poured into 180 mL of 98% sulfuric acid and 20 mL of 85% orthophosphic acid with stirring. Nine grams of potassium permanganate was then added in a slow manner. The temperature of the final solution was below 35–40°C. The solute was stored at a temperature of 50°C for 12 h and diluted carefully with 10 mL H_2O_2 (30%). After the solution was cooled, it was dissolved with H_2SO_4 (5%) taken in the same volume as the cooled solution. Ten grams of $H_2C_2O_4$ was gradually added to the blend with stirring, and the solution changed color from dark brown to pail green. After this, the blend was stored for 12 h at a temperature of 50°C, transforming into a yellow-brown solution that was subjected to 30 min of the multiple room-temperature centrifugation at a rate of 6000 rpm. The supernate was poured out after each centrifugation, and the precipitation was rinsed with distilled water and reexposed to centrifugation. The process was stopped when the pH of the supernate reached 6–7. The sample was further exposed to 2 days of sublimation drying on a Labconco 7948030 (United States) sublimator at a pressure of 0.7 mbar in a temperature range of –20 to +20°C.

Preparation of $Fe_3O_4(Na_3C_6H_5O_7)$ iron oxide. Magnetic Fe_3O_4 iron oxide nanoparticles were obtained in accordance with the technique [9]. For this, 2.234 g of $FeSO_4 \cdot 7H_2O$ and 4.348 g of $FeCl_3 \cdot 6H_2O$ salts were solved in 17 mL of water. After that, 180 mL of 4% ammonium solution was added in the blend, which immediately acquired a black color. The

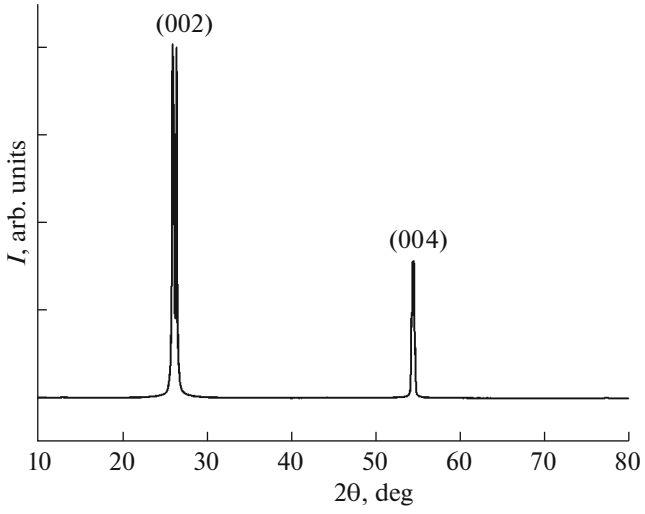

Fig. 2. X-ray diffractogram of medium-flake graphite.

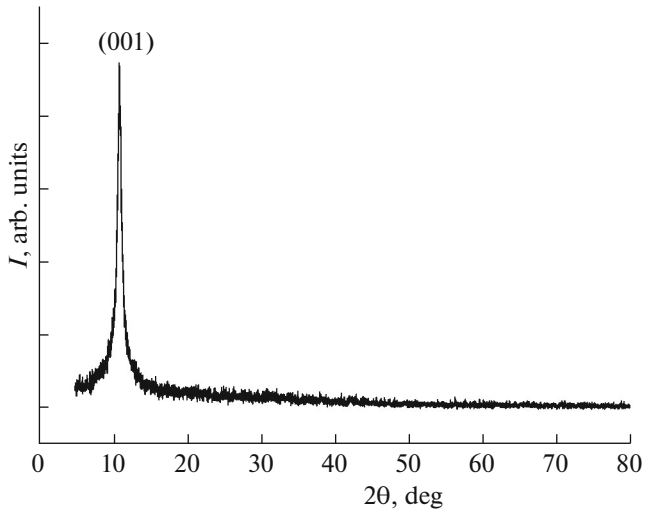

Fig. 3. X-ray diffractogram of graphite oxide synthesized by the modified method.

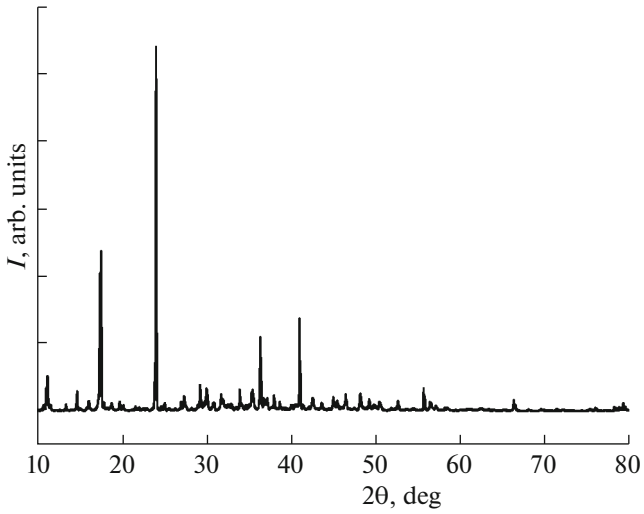

Fig. 4. X-ray diffractogram of Fe_3O_4, produced using sodium citrate.

particles in the resulting solution were appreciably attracted to the magnet. In order to stabilize them, 45.2 g of $Na_3C_6H_5O_7 \cdot 2H_2O$ diluted in 200 mL distilled water was added to the solute, which was then subjected to 30 min of heating to 80°C in continuous stirring. The final solution was placed in an ultrasonic bath for 20 min to disperse the magnetic particles.

Synthesis of DOX@Fe_3O_4 composite. In order to find the optimal composition based on doxorubicin and iron oxide, various composites were studied in the present work (Table 1).

The required compositions were obtained by adding the DOX solution to the corresponding volume of iron oxide nanoparticles and exposed to 10 min of ultrasonic treatment. The solutions were rich orange.

Synthesis of DOX@GO composite. The DOX@GO sample was prepared by mixing 15 mg of DOX with 75 mL of GO solution (1.66 M), and the solute was then adjusted to a volume of 15 mL with a phosphate buffer solution (pH 7.5). The final solution was placed onto a magnetic stirrer for 12 h at room temperature.

Synthesis of GO@Fe_3O_4@DOX. A GO@Fe_3O_4@DOX sample was prepared by mixing 75 μL of GO and 274 mL of Fe_3O_4 solution with 15 mg of DOX powder (the DOX/Fe_3O_4 weight ratio was 82/18). The mixture volume was adjusted to 15 mL with a phosphate buffer solution (pH 7.5) and was placed on a magnetic stirrer for 12 h at room temperature.

In order to inspect the behavior of the DOX in a composite containing graphite oxide and iron oxide, a solute of doxorubicin was prepared in a phosphate buffer solution (pH 7.5). The DOX concentration in the buffer was 1 mg/mL. The reference sample was produced in 15 mL of the phosphate buffer solution by diluting 15 mg of doxorubicin with adding 274 μL of the Fe_3O_4 solution with a concentration of 0.012 g/mL and 1.5 mg of graphite oxide (the DOX/Fe_3O_4 weight ratio was 82/18 because of the confirmed presence of doxorubicin in the composite for this composition). The sample was then treated in an ultrasonic bath for 20 min.

Characterization methods. Optical absorption spectra were recorded on a PerkinElmer Lambda 950 (PerkinElmer, United States) scanning UV/Vis/nIR spectrophotometer.

The electron diffraction analysis and thorough inspection of the microsctructure were conducted via transmission electron microscopy (TEM) on a LEO 912 AB Omega microscope with a LaB_6 cathode at an accelerating voltage of 100 kV (Carl Zeiss, Germany). The electron diffraction patterns were acquired with a 265-mm-long camera using metal gold as a reference.

Thermogravimetric analysis (TGA) and differential thermal analysis (DTA) were implemented on a Netzsch STA 409 PC/PG (Netzsch, Germany) thermoanalytical installation in air in platinum crucibles over a temperature range of 40–800°C at a heating rate of 5°C/min (the sample weight was 20–40 mg).

The X-ray diffraction (XRD) study was performed on a Rigaku D/MAX 2500 (Rigaku, Japan) diffractometer in the Bragg–Brentano geometry with a rotating anode (Cu$K\alpha$ radiation). The diffractograms were recorded in the step scan mode in the angle range of $2\theta = 2°–80°$ with a 2θ increment of 0.02° at an exposure time of 2 s per point. The data were processed using the conventional WinXpow software package.

The Raman spectroscopy measurements were made on an InVia Reflex (Renishaw, Great Britain) spectrometer in the confocal mode using a red He/Ne laser (excitation wavelength of 632.8 nm and power of 20 mW) and a green Ar laser (wavelength of 514.4 nm

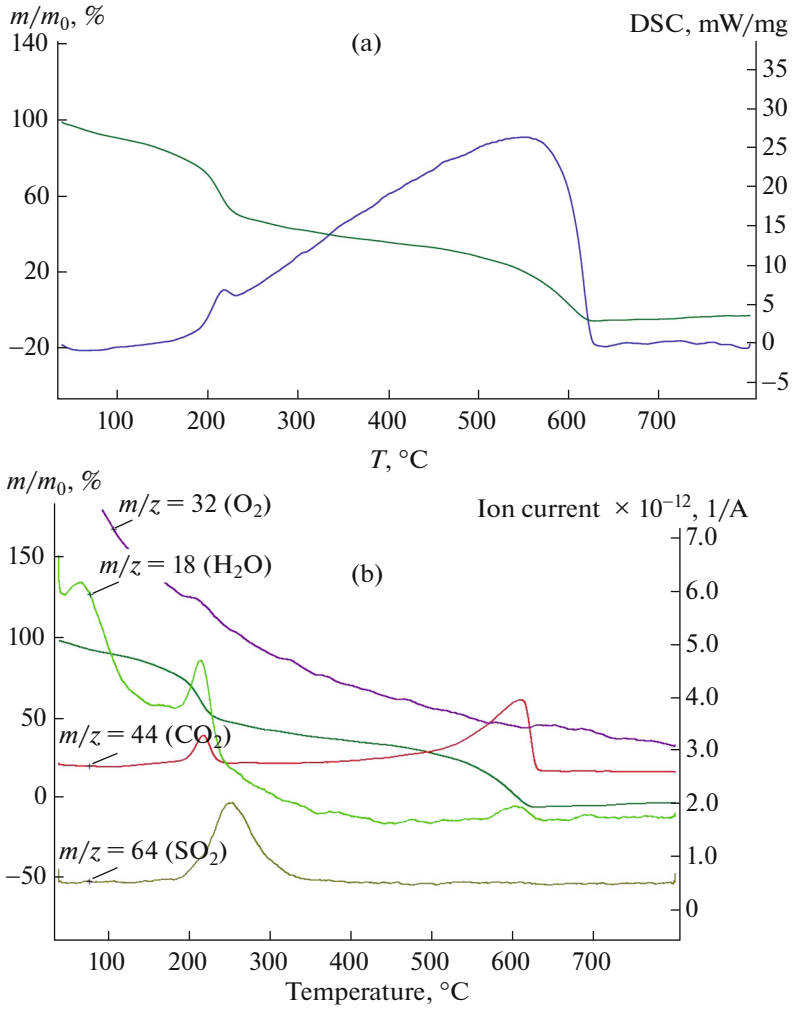

Fig. 5. (Color online) (a) TGA and DSC and (b) mass spectroscopy data of graphite oxide.

and power of 50 mW). The neutral density filter power for spectra was 100%. The acquisition time was 10 s. The setup was aligned using single-crystal silicon slabs as the reference. The Raman spectra were recorded over a wavenumber range of 100–3200 cm^{-1}. The laser power was controlled by the light-absorbing filers in the optical path.

The magnetic experiments were carried out on a Faraday balance magnetometer fabricated at the Institute of Solid State Chemistry of the Ural Branch of the Russian Academy of Sciences. For this, the Fe_3O_4 nanoparticle solution with a concentration of 0.012 g/mL was used. The magnetization of the sample was measured at a temperature of $T = 293$ K at various values of the magnetic field during the field sweep from 0 to 15000 Oe, from 15000 to −15000 Oe, and from 15000 to 15000 Oe (in the hysteresis loop acquisition mode). The precision of the magnetic moment measure was 3%, and the accuracy in determining the applied magnetic field was ±100 Oe.

RESULTS AND DISCUSSION

X-ray diffraction analysis. The X-ray spectrogram of the precursor of medium-flake graphite (Fig. 2) exhibits a high-intensity (002) signal at $2\theta = 26.2°$, which corresponds to the interplane distance of 3.4 Å. The X-ray diffractogram of GO evidences a lack of the reflex at $2\theta = 26.2°$ and the emergence of a peak at $2\theta = 10.3°$, which indicates graphite oxidation and an increase in the interplay distance to 8.6 Å in the sample, caused by the embedding of oxygen-containing groups and water molecules (Fig. 3). The pronounced broadening of (001) reflex for GO evidences a relatively small coherent domain (CD) size in the direction normal to the sheet plane.

The X-ray diffraction analysis of iron oxide (Fig. 4) reveals that the sample is not single phase and, as well as the Fe_3O_4 phase, it contains FeOOH. Nevertheless, this impurity phase does not contradict the goal of the present work, because FeOOH is also known by its magnetic properties and can be used for the creation of a composite with doxorubicin and graphite oxide.

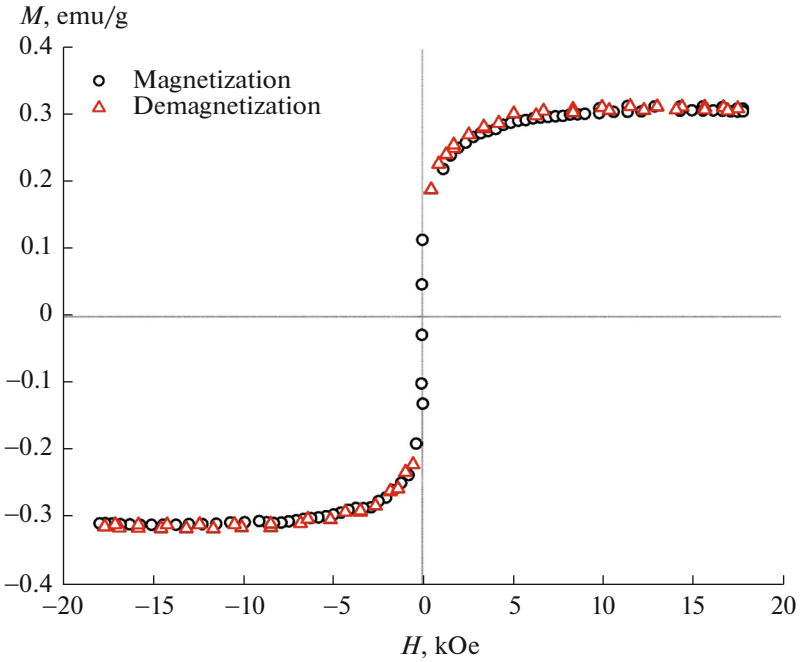

Fig. 6. (Color online) Hysteresis loop of the Fe_3O_4 sample.

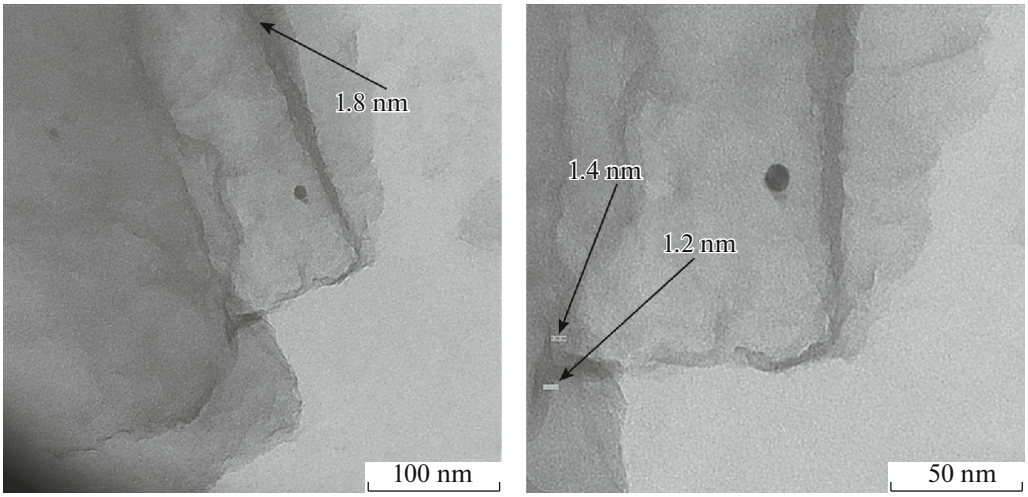

Fig. 7. TEM image of GO from dispersion in propanol-2 (0.0001 g/mL).

Thermogravimetry data. The TGA curve of the GO sample during heating from 40 to 800°C evidences two main stages of weight loss. The first one ends at around 200°C and is accompanied with a slight exoeffect. The weight loss in this temperature range is about 30%, and, according to the mass-spectrometry data of releasing gases, the main products are water, CO_2, and SO_2. The presence of gaseous sulfur oxide seems to be due to the chemical prehistory of synthesized GO, because its production involved high amounts of concentrated sulfuric acid. The second stage ends at approximately 550°C and manifests itself by a pronounced exoeffect with the release of carbon dioxide and monoxide and a weight loss of 80% of the initial value. The heating of the GO sample to 800°C results in a total weight loss of 91.2% (Fig. 5). Since carbon is the basic component of the sample, the DSC curves and temperature dependence of the release of carbon dioxide are almost identical.

Magnetic properties. The saturation magnetization $M(H)$ normalized to the sample weight as a function of the field for the magnetic liquid of iron oxide exhibits reversible and nonlinear behavior, and the remain polarization is almost zero (Fig. 6). Both these facts

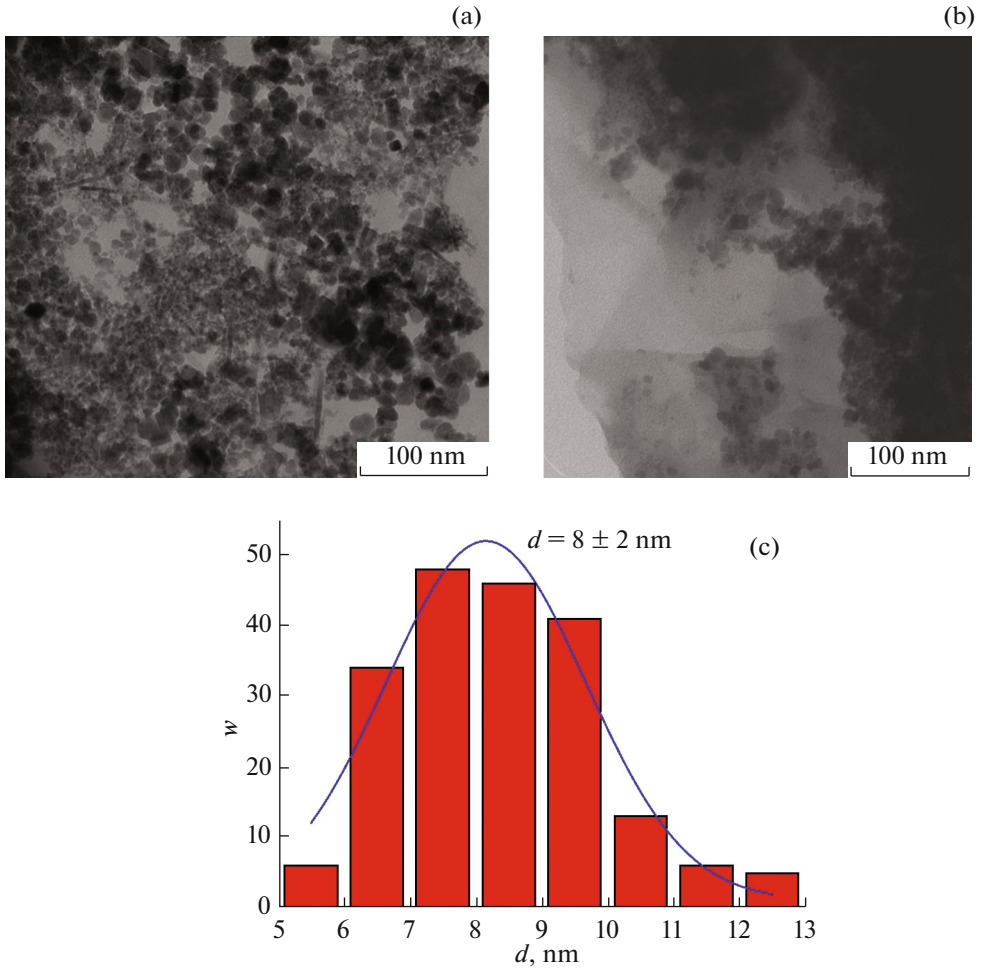

Fig. 8. (Color online) Transmission electron microscopy (TEM) data of (a) Fe_3O_4, (b) GO@Fe_3O_4@DOX, and (c) statistical processing of optical micrographs of the Fe_3O_4 sample.

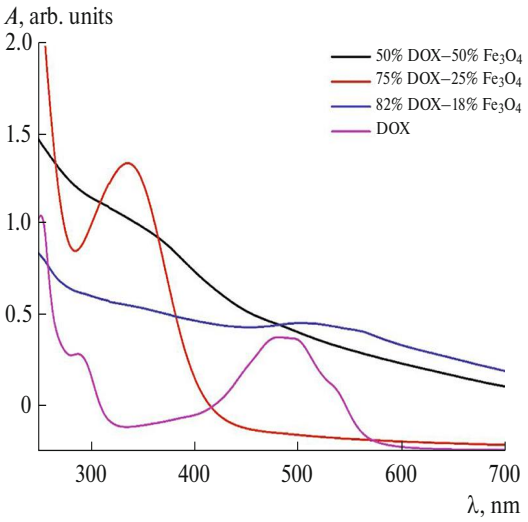

Fig. 9. (Color online) Optical absorption spectra of doxorubicin and iron oxide solutions in various ratios.

unequivocally confirm the production of Fe_3O_4-containing superparamagnetic nanoparticles.

Transmission electron microscopy. As is seen from TEM optical micrographs, the thickness of individual GO sheets is from 2 to 18 nm, which corresponds to approximately 50 layers in the sample (Fig. 7). The dark spots in micrographs are assumed to be the traces of manganeze dioxide not completely removed during the rinsing of the sample. It is thus natural that MnO_2 nanoparticles remained invisible for XRD.

It is obvious from TEM images of iron oxide and the GO@Fe_3O_4@DOX composite that Fe_3O_4 nanoparticles are composed of well-faceted cubic crystallites with an average size of about 8 nm (Fig. 8).

UV-visible spectroscopy data. Optical spectroscopy is a powerful tool for the analysis of doxorubicin-containing composites, thanks to the fact that pure doxorubicin exhibits the absorption maxima at 480 and 500 nm. The inspection of absorption spectra of 50% DOX–50% Fe_3O_4 and 75% DOX–25% Fe_3O_4 sam-

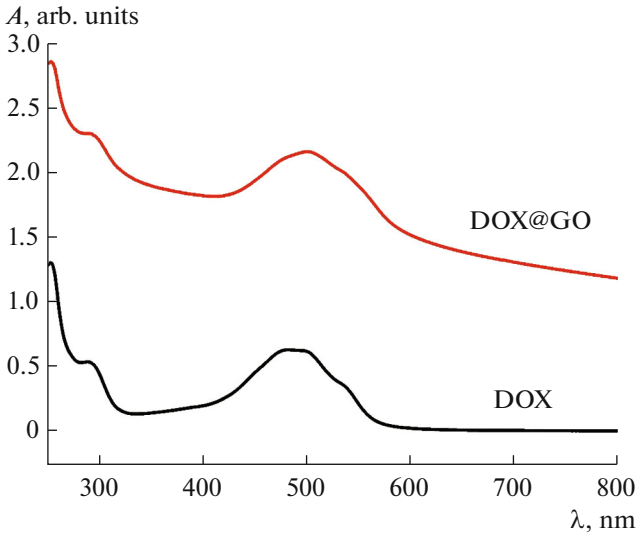

Fig. 10. (Color online) Optical absorption spectra of (a) pure doxorubicin solutions and (b) doxorubicin–graphite oxide composite.

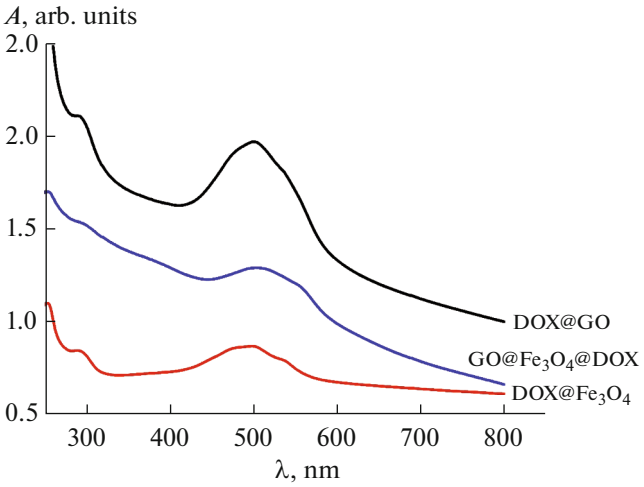

Fig. 11. (Color online) Optical absorption spectra of solutions of double and triple composites containing doxorubicin, iron oxide, and graphite oxide.

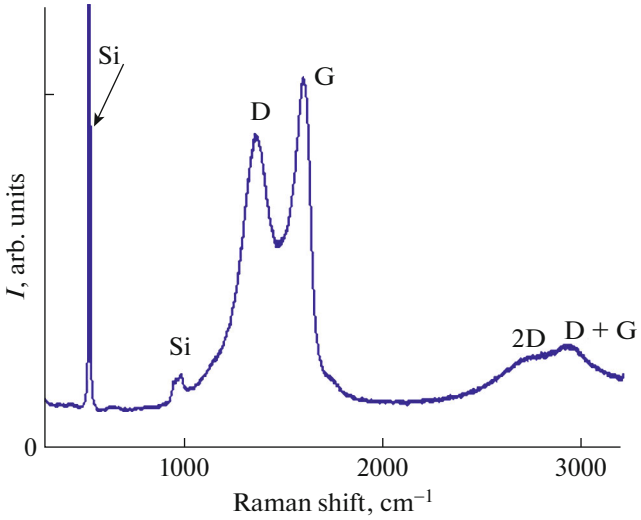

Fig. 12. (Color online) Raman spectrum of GO synthesized via the modified Hammers method.

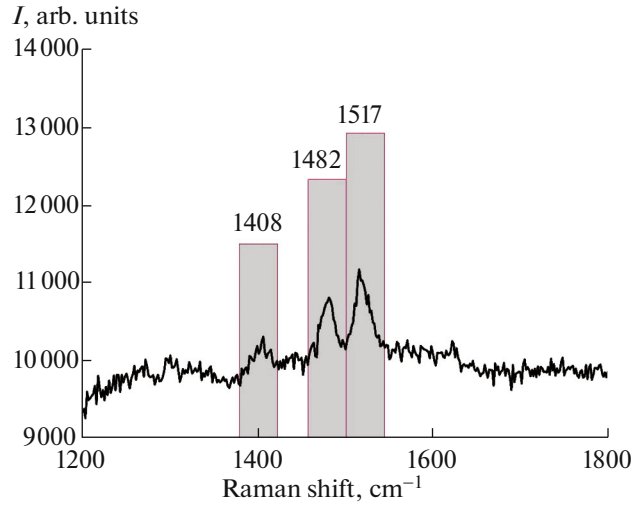

Fig. 13. (Color online) Raman spectrum of the $DOX@Fe_3O_4$ composite.

ples reveals no absorption maxima that could be typical of doxorubicin, indicating a lack of DOX in these composites. A blurred maximum at 600 nm arises in a 82% DOX–18% Fe_3O_4 composite (Fig. 9), evidencing the formation of doxorubicin complexes with Fe^{3+} ions, as follows from [18]. One can therefore assume that the formation of doxorubicin complexes with iron oxide takes place at the weight ratio of 82/18.

An analysis of the optical absorption spectra of doxorubicin composites with GO in the ratio of DOX (15 mg)–GO (1.5 mg) confirms the formation of the composite and encapsulation of doxorubicin into a GO shell, because of the similarity of spectra from pure DOX and composite (Fig. 10).

Figure 11 displays optical spectroscopy data acquired on triple and double doxorubicin-containing composites.

All absorption maxima of doxorubicin are observed in the presented spectral data. This means that one makes it possible to create not only double composites based on doxorubicin and graphite or iron oxides, but also more complex triple systems composed of magnetic nanoparticles, graphite oxide, and doxorubicin. These materials retain the specific physical and chemical properties in accordance with their components.

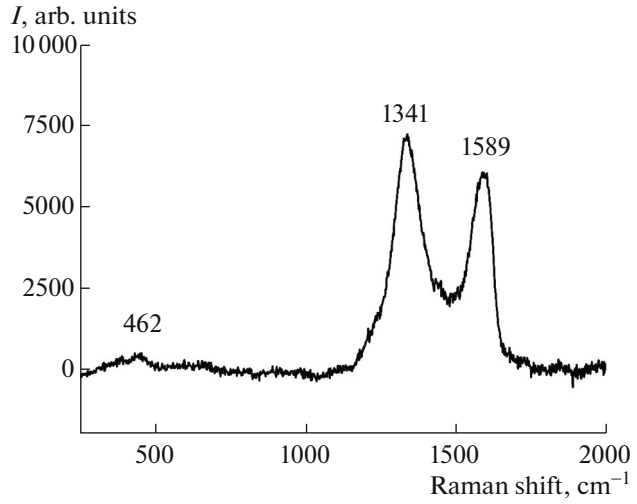

Fig. 14. Raman spectrum of GO@DOX (I_D/I_G = 7265/6098 = 1.19).

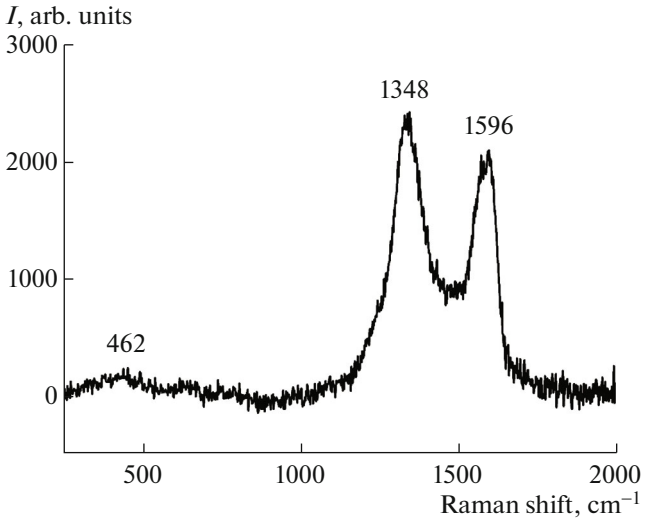

Fig. 15. Raman spectrum of GO@Fe_3O_4@DOX (I_D/I_G = 2429/2097 = 1.16).

It is worth noting that aqueous GO@Fe_3O_4@DOX composite solutions in the phosphate buffer are quite stable (there are no visible changes in a sample after one month), which makes them promising for practical use.

Raman spectroscopy is the most sensitive to high-symmetry covalent bonds with a small or missing dipole moment. Since the C–C bonds are entirely in accordance with this criterion, Raman spectroscopy is able to detect any of the finest structural changes in GO, being thus a highly valuable method for this study.

Figure 12 shows a Raman spectrum of graphite oxide applied onto a silicon slab, where the characteristic bands of a Si-substrate arise at 521.5 cm^{-1}. There are also modes typical of graphene oxide and other carbon materials, such as G (1596 cm^{-1}) and D (1358 cm^{-1}). The 2D band range exhibits several peaks (2D, D + G), which evidence the incomplete structure and the presence of defects. Both bands are due to second-order resonant Raman scattering. This is a fundamental difference between graphite oxide and graphene, which gives the pronounced bands (G and 2D) at 1580 and 2690 cm^{-1} at a low-intensity D mode.

The I_D/I_G area ratio of spectral components can be considered the sp^2/sp^3 carbon fraction ratio in the material. Thus, the intensity ratio is inversely proportional to the domain size of graphene sheets and is directly proportional to the defect concentration. For the graphite oxide used in this work, the I_D/I_G ratio is 0.88.

The Raman spectrum of doxorubicin/iron oxide composites (82/18, wt %) includes the characteristic bands of the drug, whose positions match those reported in the literature (Fig. 13), evidencing the presence of DOX in the double composite. The results are consistent with UV-visible spectroscopy data and confirm the formation of double DOX@Fe_3O_4 composite (Fig. 13).

It is worth mentioning that the Raman lines of doxorubicin at 1408–1517 cm^{-1} cover the range of D and G bands that are intrinsic of graphite oxide. Therefore, in the case of GO@DOX and GO@Fe_3O_4@DOX composites with graphite oxide, the presence of doxorubicin can be concluded from bands arising at lower wavelengths, e.g., from a line at 462 nm associated with –C–C=O bond, which is characteristic of doxorubicin as well (Figs. 14, 15).

The Raman spectra of doxorubicin encapsulated in graphite oxide and being part of the triple composite contain the characteristic band of doxorubicin at 462 nm, which proves the presence of the drug in the composite with graphite and iron oxides. Furthermore, the I_D/I_G ratio increases to a large extent in comparison with initial graphite oxide, testifying to the additional transition of some carbon atoms to the sp^3-hybridization state. This phenomenon can refer to the formation of bonds between carboxyl groups in graphite oxide and aminogroups in doxorubicin, which is expected to improve the stability of the triple composite.

CONCLUSIONS

A GO@Fe_3O_4@DOX triple composite based on graphite oxide, an iron oxide nanoparticle, and the drug doxorubicin was produced in the present work. Since it combines magnetic and drug components, this material is considered bifunctional. Graphite oxide with a biocompatible surface contains a large number of functional groups that favor chemical cou-

pling with the doxorubicin antibiotic. Superparamagnetic iron oxide particles are suitable for the hyperthermic treatment of oncological diseases and the targeted delivery of doxorubicin in the external magnetic field immediately to the affected organ. In the future, the use of the proposed nanocomposite will allow the controllable delivery of doxorubicin, and negative effects on the body will thereby be reduced.

ACKNOWLEDGMENTS

This work was supported by the Russian Federation for Basic Research (project no. 16-08-00706).

REFERENCES

1. A. K. Geim and K. S. Novoselov, "The rise of graphene," Nat. Mater. **6**, 183–191 (2007).
2. M. Hakimi and P. Alimard, "Graphene: synthesis and applications in biotechnology—a review," World Appl. Program. **2**, 377–388 (2012).
3. S. Goenka, V. Sant, and S. Sant, "Graphene-based nanomaterials for drug delivery and tissue engineering," J. Control. Release **173**, 75–88 (2014).
4. A. Bianco, H. M. Cheng, T. Enoki, Yu. Gogotsi, R. H. Hurt, N. Koratkar, T. Kyotani, M. Monthioux, C. R. Park, J. M. D. Tascon, and J. Zhang, "All in the graphene family—a recommended nomenclature for two-dimensional carbon materials," Carbon **65**, 1–6 (2013).
5. D. C. Marcano, D. V. Kosynkin, J. M. Berlin, A. Sinitskii, Z. Sun, A. Slesarev, L. B. Alemany, W. Lu, and J. M. Tour, "Improved synthesis of graphene oxide," ACS Nano **4**, 4806–4814 (2010).
6. A. L. Higginbotham, D. V. Kosynkin, A. Sinitskii, Z. Sun, and J. M. Tour, "Lower-defect graphene oxide nanoribbons from multiwalled carbon nanotubes," ASC Nano **4**, 2059–2069 (2010).
7. J. Liu, L. Cui, and D. Losic, "Graphene and graphene oxide as new nanocarriers for drug delivery applications," Acta Biomater. **9**, 9243–9257 (2013).
8. S. A. Shah, M. U. A. Khan, M. Arshad, S. U. Awan, M. U. Hashmi, and N. Ahmad, "Doxorubicin-loaded photosensitive magnetic liposomes for multi-modal cancer therapy," Colloids Surf., B **148**, 157–164 (2016).
9. J. Gautier, E. Allard-Vannier, E. Munnier, M. Soucé, and I. Chourpa, "Recent advances in theranostic nanocarriers of doxorubicin based on iron oxide and gold nanoparticles," J. Control. Release **169**, 48–61 (2013).
10. W. Zhang, Z. Guo, D. Huang, Z. Liu, X. Guo, and H. Zhong, "Synergistic effect of chemo-photothermal therapy using PEGylated graphene oxide," Biomaterials **32**, 8555–8561 (2011).
11. Z. Wang, C. Zhou, J. Xia, B. Via, Y. Xia, F. Zhang, Y. Li, and L. Xia, "Fabrication and characterization of a triple functionalization of graphene oxide with Fe_3O_4, folic acid and doxorubicin as dual-targeted drug nanocarrier," Colloids Surf., B **106**, 60–65 (2013).
12. E. Munnier, S. Cohen-Jonathan, C. Linassier, L. Douziech-Eyrolles, H. Marchais, M. Souce, K. Herve, P. Dubois, and I. Chourpa, "Novel method of doxorubicin—SPION reversible association for magnetic drug targeting," Int. J. Pharm. (Amsterdam, Neth.) **363**, 170–176 (2008).
13. W. Zhang, X. Zheng, S. Shen, and X. Wang, "Doxorubicin-loaded magnetic nanoparticle cluster for chemo-photothermal treatment of the prostate cancer cell line PCl_3," Biochem. Biophys. Res. Commun. **466**, 278–282 (2015).
14. X. Yang, J. J. Grailer, I. J. Rowland, A. Javadi, S. A. Hurley, D. A. Steeber, and S. Gong, "Multifunctional SPIO/DOX-loaded wormlike polymer vesicles for cancer therapy and MR imaging," Biomaterials **31**, 9065–9073 (2010).
15. J. Gupta, A. Prakash, M. K. Jaiswal, A. Agarrwal, and D. Bahadur, "Superparamagnetic iron oxide-reduced graphene oxide nanohybrid-a-vehicle for targeted drug delivery and hyperthermia treatment of cancer," J. Magn. Magn. Mater. **448**, 332–338 (2018).
16. A. Semkina, M. Abakumov, N. Grinenko, A. Abakumov, A. Skorikov, E. Mironova, G. Davydova, A. G. Majouga, N. Nukolova, A. Kabanov, and V. Chekhonin, "Core–shell–corona doxorubicin-loaded superparamagnetic Fe_3O_4 nanoparticles for cancer theranostics," Colloids Surf., B **136**, 1073–1080 (2015).
17. M.-M. Song, H.-L. Xu, J.-X. Liang, H.-H. Xiang, R. Liu, and Y.-X. Shen, "Lactoferrin modified graphene oxide nanocomposite for glioma–targed drug delivery," Mater. Sci. Eng. C **77**, 904–911 (2017).

Translated by O. Maslova